

Anisotropic and enhanced absorptive nonlinearities in a macroscopic film induced by aligned gold nanorods

Jiafang Li,^{a)} Siyun Liu, Ye Liu, Fei Zhou, and Zhi-Yuan Li^{a)}

Laboratory of Optical Physics, Institute of Physics, Chinese Academy of Sciences, Beijing 100190, People's Republic of China

(Received 12 May 2010; accepted 8 June 2010; published online 29 June 2010)

Anisotropic and enhanced nonlinear absorption (NLA) has been observed from aligned gold nanorods (GNRs) embedded in a poly(vinyl alcohol) film, which was realized by a stretched-film method. Open-aperture Z-scan experiments revealed that the stretch process enhanced the NLA coefficient by approximately nine times and increased the anisotropic factor of NLA to ~ 20 . The enhancement in the NLA coefficient reached as high as ~ 91 times after increasing the concentration of GNRs by four times and this is attributed to the plasmonic interaction between densely packed GNRs. © 2010 American Institute of Physics. [doi:10.1063/1.3458693]

Gold nanorods (GNRs) have attracted great interest^{1–6} due to their anisotropic splitting of the surface plasmon resonance (SPR) into two polarization-dependent components, i.e., the transverse (TSPR) and the longitudinal (LSPR) component. Compared with the weak TSPR around 530 nm, the LSPR of GNRs induces strong absorption, scattering, local-field enhancement, and photoluminescence. Consequently, GNRs have appealing applications in surface enhanced Raman spectroscopy, biological imaging and sensing, photothermal therapy, optical data encoding, etc.^{4,7–9} However, in most applications, only a portion of the GNRs with certain orientations was utilized because GNRs are naturally randomly oriented and their LSPR cannot be excited in the direction perpendicular to their longitudinal axes. Moreover, the random distribution averages the microscopic anisotropy of the single GNR and the assembled GNRs behave like macroscopically isotropic materials. Therefore, macroscopically representing or constructively amplifying the anisotropic optical properties of a single GNR could be very preferable to improve the efficiency of GNR applications. For example, it was predicted that assembling GNRs into ordered structures can achieve very large optical nonlinearities.¹⁰

Here we demonstrate the anisotropic and enhanced nonlinear absorption (NLA) from aligned GNRs in a poly(vinyl alcohol) (PVA) film, which was realized by utilizing a well-developed stretched-film method.^{11–14} Specifically, the stretch process directly enhanced the NLA coefficient of the film by approximately nine times. It was further observed that the absorptive nonlinearities of the aligned GNRs in PVA films were more than the linear summation of the nonlinearities of individual GNRs. Compared with a non-stretched film, an increase in the GNR concentration by four times in the stretched GNRs/PVA film could enhance the NLA coefficient by ~ 91 times.

For sample preparation, GNRs water solution was synthesized by using a seed-mediated growth method.¹ The dimensions of the GNRs [as shown in Fig. 1(a)] were controlled by adding different amounts of AgNO_3 . After the synthesis, the GNRs were purified and mixed with a 15% aqueous PVA solution by a volume ratio of 1:1. GNRs/PVA

films were prepared by pouring the mixture into a Petri dish and then drying the samples naturally for 24 h at room temperature, which resulted in uniform polymer films with a thickness of $\sim 100 \mu\text{m}$ (dependent on the amount of the mixture used). Finally, the GNRs/PVA films were cut into a rectangular shape and manually stretched in one direction under heating at $\sim 65^\circ\text{C}$ [as schematically shown in Fig. 1(b)] until a desired length was obtained. In our experiments, the final length of the stretched film was chosen to be approximately five times of its original length, which ensures the nearly complete alignment of GNRs inside the stretched films.¹¹

During the stretch process, the PVA molecules elongate along the stretch direction, which causes the longitudinal axes of GNRs orienting along the stretch direction.¹⁴ Because the LSPR mode is inherently polarized along the longitudinal axis, the stretched films will show collective LSPR when the incident light is polarized parallel to the stretch direction. In such a way, the stretched film could macroscopically enact the anisotropic optical properties of a single

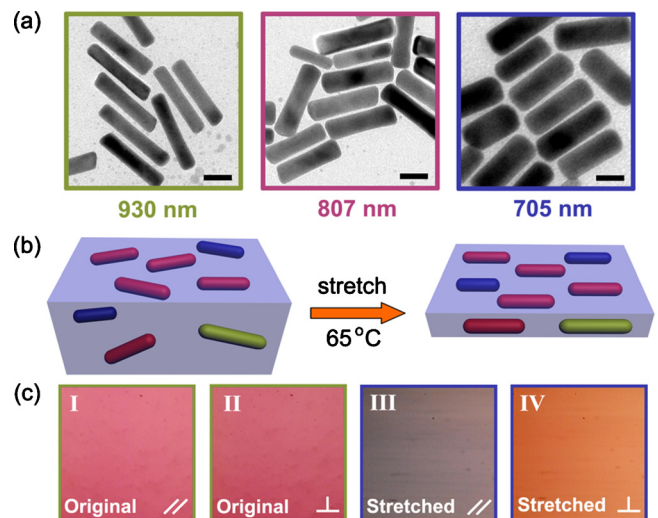


FIG. 1. (Color online) (a) TEM images of synthesized GNRs with LSPR wavelengths as noted. Scale bars: 20 nm. (b) Schematic diagram of the stretched-film process. (c) Optical microscopy images of the original and stretched film under white light illumination with polarization parallel (\parallel) and perpendicular (\perp) to the stretch direction.

^{a)}Authors to whom correspondence should be addressed. Electronic addresses: jiafangli@aphy.iphy.ac.cn and lizy@aphy.iphy.ac.cn.

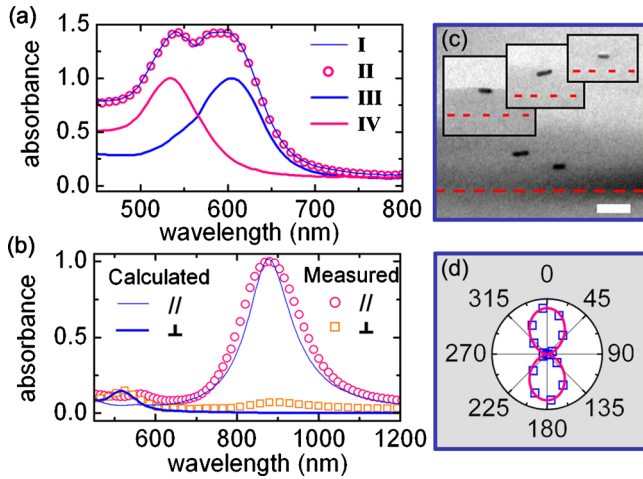


FIG. 2. (Color online) (a) Measured absorbance spectra of the GNRs/PVA films corresponding to Fig. 1(c). Spectra were normalized and vertically shifted for clear display. (b) Measured absorbance spectra of another stretched GNRs/PVA film under excitation polarized parallel (\parallel) and perpendicular (\perp) to the stretch direction. Solid lines are the corresponding calculations of a single GNR. (c) TEM images of the aligned GNRs in the PVA film. Scale bar: 100 nm. Dashed lines indicate the direction of stretch. (d) Polar plot of the measured absorption intensity at wavelength 800 nm vs the excitation polarization angle. The solid curve is a fit to the cosine squared function.

GNR. As shown in Fig. 1(c), a stretched GNRs/PVA film shows distinct colors when the incident light is polarized parallel and perpendicular to the stretch direction, respectively, while the original film shows the same color in both polarization directions. These color displays are inherently associated with the corresponding absorption spectra. As shown in Fig. 2(a), the original film shows two absorption peaks irrespective of the light polarization directions (curves I and II). After the stretch, the film possesses only one absorption peak upon each polarized excitation, which corresponds to the LSPR (curve III) and TSPR (curve IV), respectively. This splitting of the LSPR and TSPR in the macroscopic films could find useful applications in polarization-dependent color display devices.⁴

For nonlinear enhancement experiments, we employed GNRs with large aspect ratios (~ 4), of which the LSPR and TSPR were well separated, as shown in Fig. 2(b). The measured SPR peaks matched well with the calculation of a single GNR. Notably, the linewidth of the LSPR peak was close between theory for a single GNR and experiment for a macroscopic assembly of GNRs, which indicates the narrow size distribution and the well alignment of GNRs. The small difference between the measurements and calculations were caused by the deviation from the perfect GNR alignment, which was about 7% judged from the absorbance intensity. The alignment of GNRs was also confirmed by transmission electron microscopy (TEM) images of the stretched GNRs/PVA film, as shown in Fig. 2(c). The anisotropic absorption properties of the stretched GNRs/PVA film are further illustrated in Fig. 2(d), where the experimental data from the macroscopic film were well fitted using a cosine squared function that represents the anisotropic properties of a single GNR.³

The absorptive nonlinearities of various GNRs/PVA films were investigated by using the standard open-aperture Z-scan technique [Fig. 3(a)].¹⁵ In the experiments, a pulsed laser (pulse width 3 ns) with a wavelength of 800 nm and a

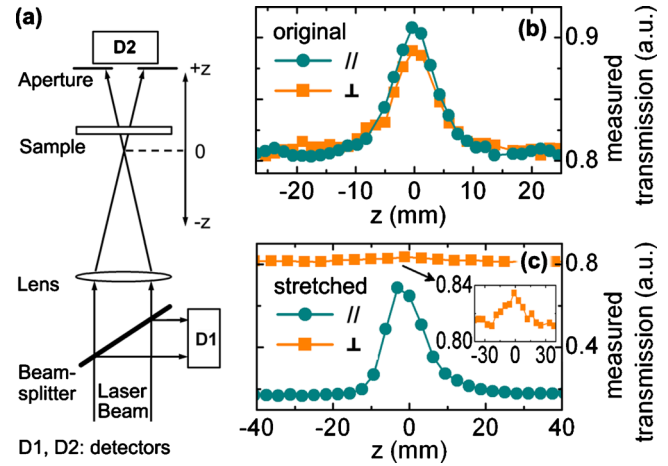


FIG. 3. (Color online) (a) Schematic diagram of the Z-scan setup (reported in Ref. 15). (b)(c) Measured transmission of (b) nonstretched and (c) stretched GNRs/PVA films upon laser excitation polarized parallel (\parallel) and perpendicular (\perp) to the stretch direction, respectively. Inset: Rescaled plot of the curve noted by the arrow. GNR concentrations (C_{GNR}) of the films: (b) 3.75 nmol/L and (c) 15 nmol/L.

repetition rate of 10 Hz was used as the excitation source. After expansion, the laser beam was focused by a lens with a beam waist of $\sim 15 \mu\text{m}$ onto the sample. While the samples were kept moving around the focus, the on-axis transmitted beam energy and the reference beam energy were measured simultaneously by an energy ratiometer (Rm 6600, Laser Probe Corp.).

The measured open-aperture Z-scan transmission curves are presented in Figs. 3(b) and 3(c). As expected, the original GNRs/PVA film showed similar transmission responses upon the excitation with two different polarizations [Fig. 3(b)]. While the linear absorption dominated in the region that was far away from the focus ($|z| > 20 \text{ mm}$), the transmission peaks appearing at $z=0$ were caused by the absorption saturation of the GNRs because of the high laser intensity near the focus.¹⁶ For a stretched film, on the other hand, there was a big difference in the Z-scan curves. In the case of parallel-polarized excitation, the NLA effects were very obvious while for the perpendicular-polarized excitation the NLA effects were very weak and difficult to characterize even after increasing the GNR concentration by four times [Fig. 3(c)]. The polarization independent and dependent transmission curves in Fig. 3(b) and Fig. 3(c) clearly illustrate the anisotropic nonlinear effects induced by the alignment of GNRs.

To quantify the absorptive nonlinearity of our samples, the experimental data were normalized (to remove the effects of linear absorption) and fitted by using the Z-scan equation $T(z) = \sum_{m=0}^{\infty} (-q_0)^m / (1 + z^2/z_0^2)^{(m+1)^{3/2}}$,¹⁵ where $q_0 = \beta I_0 L_{\text{eff}}$, β is the NLA coefficient, I_0 is the laser intensity at the focus, and L_{eff} is the effective thickness of the sample defined by $L_{\text{eff}} = (1 - e^{-\alpha L}) / \alpha$ with L being the sample thickness and α being the linear absorption coefficient. With the fittings, the values of β can be obtained for analysis. For example, the fitted β values in Fig. 3(b) were $\beta_{\parallel} = -2.70 \times 10^{-8} \text{ m/W}$ and $\beta_{\perp} = -2.59 \times 10^{-8} \text{ m/W}$, respectively. Therefore the macroscopic anisotropy factor of NLA can be evaluated by $\beta_{\parallel} / \beta_{\perp} = 1.04$, which indicates that this sample was nearly isotropic. Impressively, for the sample in Fig. 3(c), the anisotropic factor reached as high as ~ 20 ($\beta_{\parallel} = -7.23 \times 10^{-8} \text{ m/W}$ and $\beta_{\perp} = -0.37 \times 10^{-8} \text{ m/W}$). Such strong anisotropy in nonlinearities can be attributed to the well-

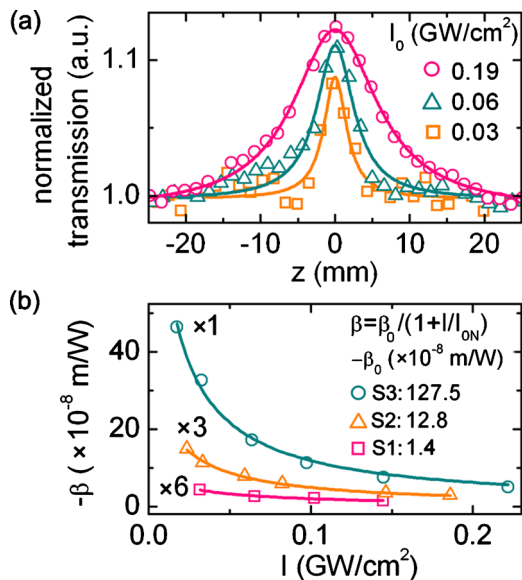


FIG. 4. (Color online) (a) Normalized transmission of a stretched GNRs/PVA film excited with different laser intensities. The laser polarization was along the stretch direction. Solid lines are corresponding fittings with the Z-scan theory (reported in Ref. 15). (b) NLA coefficient ($-\beta$) as a function of the laser intensity for three samples: (\square) S1: original film with $C_{\text{GNR}} = 3.75$ nmol/L; (\triangle) S2: stretched film with $C_{\text{GNR}} = 3.75$ nmol/L; (\circ) S3: stretched film with $C_{\text{GNR}} = 15$ nmol/L. The experimental data and their fittings (solid lines) were multiplied by corresponding numbers as noted for comparison purpose.

aligned GNRs in the stretched PVA films as well as the narrow size distribution of the colloidal GNRs.

During the analysis, it was observed that the Z-scan measurement was intensity dependent, as shown in Fig. 4(a). To ensure the accuracy in comparisons between different samples, we performed a series of intensity-dependent Z-scan measurements, deduced the corresponding β values, and fitted the obtained β data with a formula $\beta = \beta_0 / (1 + I/I_{0N})$, where β_0 is the initial NLA coefficient under low-irradiance excitation and I_{0N} is the saturation irradiance of the NLA. As plotted in Fig. 4(b), the measured β values were well fitted with the formula, from which the values of β_0 were obtained for comparisons. For samples (S1 and S2) with the same GNR concentration it showed that the value of β_0 was enhanced by approximately nine times by the simple stretch process. Moreover, it was noticed that the GNR concentration played a giant effect on the increase in β_0 value. After increasing the GNR concentration by four times, the β_0 value of the stretched film (sample S3) reached -127.5×10^{-8} m/W (corresponding to the imaginary part of third-order nonlinear susceptibility as $\text{Im} \chi^{(3)} = -4.3 \times 10^{-8}$ esu), which was about 91 times of that of the original film (S1). It should be mentioned that due to the long-duration laser pulses, the measured β values in our solid-state films ($> 10^{-8}$ m/W) were more than three orders of magnitude higher than those reported in similar GNR solutions ($\sim 10^{-11}$ m/W).¹⁶⁻¹⁸

It has been recently studied in a GNRs/silica film that in approximation $\text{Im} \chi^{(3)}$ is linearly related with the metal volume concentration ρ when $\rho \leq 1$.¹⁹ However, although the values of ρ in our samples were $\sim 0.04\%$, we obtained $(\text{Im} \chi^{(3)})_{\text{S2}} / (\text{Im} \chi^{(3)})_{\text{S3}} \approx 10$, which was 2.5 times of the ratio in concentration $\rho_{\text{S2}} / \rho_{\text{S3}} = 4$. This observation indicated that the absorptive nonlinearities of the aligned GNRs were more

than just the linear summation of the nonlinearities of individual GNR. This is reasonable because that besides the collective effects of separated GNRs, the plasmonic interaction between adjacent aligned GNRs is able to strengthen the local electric field and thus increase the NLA.¹⁹⁻²¹ Therefore, utilizing the plasmonic interactions and local field enhancement inside aligned GNRs films provides an effective way to amplify the nonlinear effects of single GNR.

In conclusion, we have demonstrated the strong anisotropy (with a factor of ~ 20) and enhancement (by a factor of ~ 9) in NLA from a GNRs/PVA film by aligning the embedded GNRs. Through utilizing the strong plasmonic interactions between adjacent GNRs, the enhancement in NLA coefficient can be further increased to ~ 91 times. The work here opened up the way to macroscopically represent and constructively amplify the optical properties of a single GNR, such as its anisotropy in nonlinearity enhancement and emission control.^{5,6} The enhanced absorptive nonlinearity can find promising applications in optical limiting, Q-switching, plasmonic waveguides, sensor protection, etc.²²⁻²⁵

This work was supported by the National Natural Science Foundation of China under Grant Nos. 60736041 and 10874238 and the National Key Basic Research Special Foundation of China under Grant No. 2006CB302901.

¹B. Nikoobakht and M. A. El-Sayed, *Chem. Mater.* **15**, 1957 (2003).

²T. K. Sau and C. J. Murphy, *Langmuir* **20**, 6414 (2004).

³P. Zijlstra, J. W. M. Chon, and M. Gu, *Nature (London)* **459**, 410 (2009).

⁴J. Pérez-Juste, I. Pastoriza-Santos, L. M. Liz-Marzan, and P. Mulvaney, *Coord. Chem. Rev.* **249**, 1870 (2005).

⁵W. H. Ni, T. Ambjornsson, S. P. Apell, H. J. Chen, and J. F. Wang, *Nano Lett.* **10**, 77 (2010).

⁶T. Ming, L. Zhao, Z. Yang, H. J. Chen, L. D. Sun, J. F. Wang, and C. H. Yan, *Nano Lett.* **9**, 3896 (2009).

⁷A. Bouhelier, R. Bachelot, G. Lerondel, S. Kostcheev, P. Royer, and G. P. Wiederrecht, *Phys. Rev. Lett.* **95**, 267405 (2005).

⁸L. Tong, Q. S. Wei, A. Wei, and J. X. Cheng, *Photochem. Photobiol.* **85**, 21 (2009).

⁹X. H. Huang, S. Neretina, and M. A. El-Sayed, *Adv. Mater. (Weinheim, Ger.)* **21**, 4880 (2009).

¹⁰M. Pelton, M. Z. Liu, S. Park, N. F. Scherer, and P. Guyot-Sionnest, *Phys. Rev. B* **73**, 155419 (2006).

¹¹B. M. I. van der Zande, L. Pages, R. A. M. Hikmet, and A. van Blaaderen, *J. Phys. Chem. B* **103**, 5761 (1999).

¹²C. L. Murphy and C. J. Orendorff, *Adv. Mater. (Weinheim, Ger.)* **17**, 2173 (2005).

¹³J. Pérez-Juste, B. Rodriguez-Gonzalez, P. Mulvaney, and L. M. Liz-Marzan, *Adv. Funct. Mater.* **15**, 1065 (2005).

¹⁴D. Fornasiero and F. Grieser, *Chem. Phys. Lett.* **139**, 103 (1987).

¹⁵M. Sheik-Bahae, A. A. Said, T. H. Wei, D. J. Hagan, and E. W. Vanstryland, *IEEE J. Quantum Electron.* **26**, 760 (1990).

¹⁶H. I. Elim, J. Yang, J. Y. Lee, J. Mi, and W. Ji, *Appl. Phys. Lett.* **88**, 083107 (2006).

¹⁷H. M. Gong, Z. K. Zhou, S. Xiao, H. Song, X. R. Su, M. Li, and Q. Q. Wang, *Chin. Phys. Lett.* **24**, 3443 (2007).

¹⁸L. De Boni, E. L. Wood, C. Toro, and F. E. Hernandez, *Plasmonics* **3**, 171 (2008).

¹⁹J. M. Lamarre, F. Billard, and L. Martinu, *J. Opt. Soc. Am. B* **25**, 961 (2008).

²⁰A. M. Funston, C. Novo, T. J. Davis, and P. Mulvaney, *Nano Lett.* **9**, 1651 (2009).

²¹C. Tabor, D. Van Haute, and M. A. El-Sayed, *ACS Nano* **3**, 3670 (2009).

²²R. West, Y. Wang, and T. Goodson, *J. Phys. Chem. B* **107**, 3419 (2003).

²³A. N. Shipway, E. Katz, and I. Willner, *ChemPhysChem* **1**, 18 (2000).

²⁴L. François, M. Mostafavi, J. Belloni, and J. A. Delaire, *Phys. Chem. Chem. Phys.* **3**, 4965 (2001).

²⁵S. A. Maier, P. G. Kik, H. A. Atwater, S. Meltzer, E. Harel, B. E. Koel, and A. A. G. Requicha, *Nature Mater.* **2**, 229 (2003).